

# CREEP OF STRUCTURAL ADHESIVES - AN OVERVIEW

**Inês COSTA**

PhD student

ISISE - University of Minho

Department of Civil Engineering, Campus de Azurém, 4800-058 Guimarães, Portugal

*ines.costa@civil.uminho.pt\**

**Joaquim BARROS**

Full Professor

ISISE - University of Minho

Department of Civil Engineering, Campus de Azurém, 4800-058 Guimarães, Portugal

*barros@civil.uminho.pt*

## Abstract

This study is part of a research project that aims to develop a new strategy to apply prestressed Carbon Fibre Reinforced Polymer (CFRP) laminates according to the Near Surface Mounted (NSM) technique for the flexural strengthening of Reinforced Concrete elements. CFRP elements exhibit lower relaxation than common steel strands and the creep of the bonding agents is, therefore, the most relevant effect to be taken into account in the long-term effectiveness of this strengthening technique. This paper describes an experimental program carried out for the assessment of the creep model that best describes the adhesive selected to be used with the NSM technique in development. From the obtained data it was verified that Burgers model is capable of simulating with high accuracy the creep behaviour of the adopted adhesive.

**Keywords:** Analytical models, Creep, Standards, Structural adhesives, Theoretical models.

## 1. Introduction

Prestressed FRPs are known to magnify the efficiency of passive FRP reinforcement, namely due to their ability of closing or reducing the width of existing cracks and delaying the appearance of new fissures, resulting in benefits in terms of structural integrity and concrete durability [1-3]. Prestressed FRPs are also much more effective than passive (non prestressed) FRPs in terms of increasing the load carrying capacity for deflection levels corresponding to service limit states. However, as for common prestressed reinforcement steel, it is necessary to quantify the prestress losses associated with this new technology, especially with regard to the time-dependent losses, which result essentially from the creep/shrinkage of the adhesive and the relaxation of the prestressing material.

While prestressed FRPs reveal low prestress losses, as a result of their relatively low elastic modulus [4], and lower stress relaxation than steel strands [5], excessive creep/shrinkage of the adhesives that transfer the stresses between FRP and concrete substrate may lead to significant losses of prestress in the FRP. Although epoxy adhesives present a certain amount of shrinkage during the curing process, this shrinkage is almost ended when complete cure is achieved [6-7] and creep becomes the most relevant phenomenon.

The primary function of the structural adhesive is to transmit as smoothly and uniformly as possible the stresses between FRP and surrounding concrete [8]. A careful bibliographic review was carried out [9] to better understand how epoxy adhesives behave over time, and revealed that the level of applied stress and the environmental exposure conditions [8], mostly temperature and humidity, are the factors that most influence the long-term performance of

the adhesive. It was also verified that most of the analytical equations presented are based on rheological models, with occasional minor adjustments. The performance of a viscoelastic material can be quite conditioned by its creep behaviour, with consequences at the material and structural levels. Due to the significant relevance of creep in adhesives, ASTM and ISO [10-11] proposed some recommendations for its characterization by experimental assessment.

## 2. Rheological Models

Structural epoxy adhesives exhibit notable viscoelastic behaviour, since their deformation under a constant stress varies significantly in time, which can compromise the capacity of stress transference from the FRP to the substrate. This viscoelastic behaviour is frequently modelled using rheological models, and is usually illustrated by means of Hookean springs (Figure 1a) and Newtonian dashpots (Figure 1b) that replicate, respectively, the elastic and viscous components of the material's behaviour [12].

There are essentially three classical rheological models, all named after their proposers: Maxwell, Kelvin and Burgers. This last model consists on the assemblage of the previous two, as depicted in Figure 2a. Therefore, the strain response of Burgers model (Figure 2b) results from the addition of the strain responses produced by Maxwell and Kelvin models, and can be expressed in mathematical terms by Eq. (1).

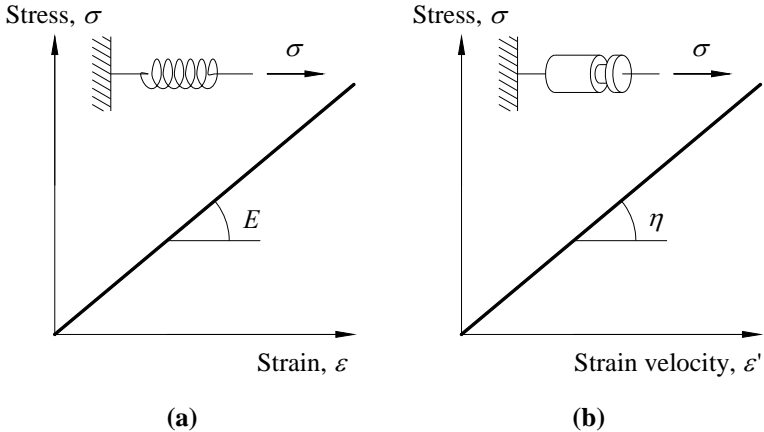


Figure 1 – Diagram of (a) linear elastic behaviour and (b) linear viscous behaviour.

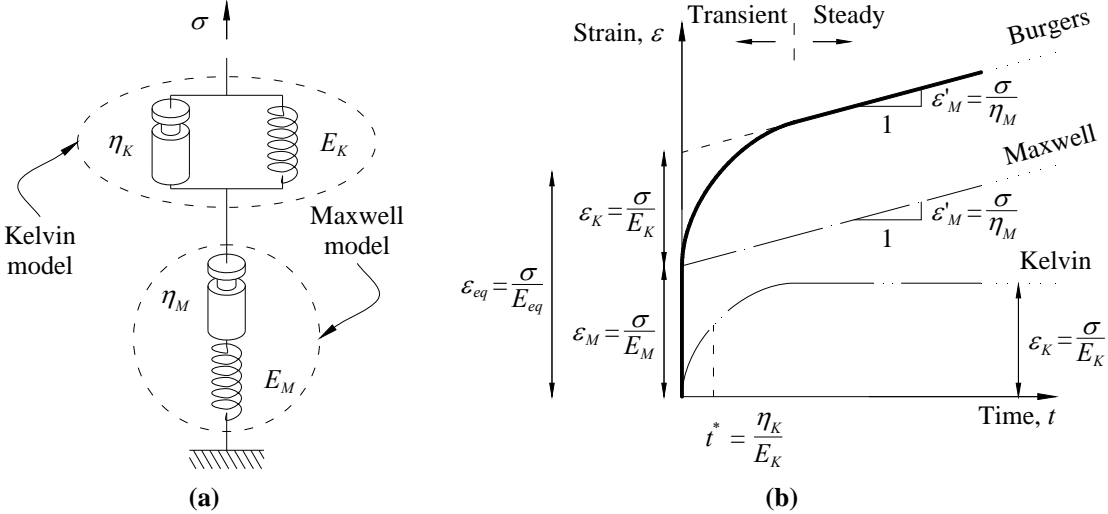


Figure 2 – Rheological models: (a) Burgers model schematization and (b) Strain response of different rheological models.

$$\varepsilon(t) = \underbrace{\frac{\sigma}{E_M} + \frac{\sigma}{\eta_M}t}_{\text{Maxwell response}} + \underbrace{\frac{\sigma}{E_K} \left(1 - e^{-\frac{E_K t}{\eta_K}}\right)}_{\text{Kelvin response}} \quad (1)$$

### 3. Experimental program

With the purpose of verifying the applicability of these rheological models to the structural adhesives to be used in prestressed FRP applications, an experimental program was carried out. The recommendations of the most significant standards [10-11] were analyzed in order to implement the most relevant ones. In short, the standards [10-11] recommend that load is applied smoothly to a standard specimen within 1 to 5 seconds and maintained for at least 1000 hours (approximately 42 days). The tests shall be repeated for an appropriate number of stress levels, for each applicable combination of temperature/humidity. In this experimental program two series of three levels of stress each were tested under a constant temperature of 20°C and constant relative humidity of 60%. In both series, the test preparation and execution was identical except for the material that, although the same, was produced from two different batches.

#### 3.1 Tensile Properties

Preliminary tensile tests, performed according to ISO 527-2 [13], revealed that the selected adhesive, at 24 hours of age, achieves a stable Young Modulus and a relatively high tensile strength (over 35 MPa), and is therefore considered as completely cured at that age. In both series executed, the fundamental tensile properties were assessed at the loading age (0 hours, which corresponds to an adhesive with 24 hours of age), and in the end of the creep tests (1000 hours), as reported in Table 1. It was noted that in terms of stiffness (Young modulus,  $E_{0.5 \sim 2.5\%}$ ), the specimens from series I developed a considerable increase from the loading instant to the end of the creep test, while the specimens of series II maintained their modulus, although with a lower tensile strength at the loading age,  $f_{max, t=0h}$ .

**Table 1. Tensile Properties of the adhesive.**

| SERIES    | $t = 0$ hours                   |                                 | $t = 1000$ hours               |                                 |
|-----------|---------------------------------|---------------------------------|--------------------------------|---------------------------------|
|           | $E_{0.5 \sim 2.5\%}$            | $f_{max}$                       | $E_{0.5 \sim 2.5\%}$           | $f_{max}$                       |
| Series I  | 5.95 GPa<br>(0.68 GPa)<br>[11%] | 41.04 MPa<br>(3.25 MPa)<br>[8%] | 6.50 GPa<br>(0.21 GPa)<br>[3%] | 46.64 MPa<br>(3.54 MPa)<br>[8%] |
| Series II | 6.14 GPa<br>(0.34 GPa)<br>[6%]  | 31.61 MPa<br>(1.41 MPa)<br>[4%] | 6.14 GPa<br>(0.28 GPa)<br>[5%] | 41.93 MPa<br>(2.46 MPa)<br>[6%] |

Average, (Standard Deviation) and [Coefficient of variation]

#### 3.2 Experimental tensile creep curves

The creep specimens used presented the same geometry adopted for tensile tests, and defined by ISO 527-2. In each series, three stress levels were applied to the standard specimens in a creep table designed to amplify 3 times a given static load, which permitted applying approximately 5, 10 and 15 MPa in each specimen (Figure 3a). However, as load was applied by means of standard weights, the real stress level installed in the specimens was also

influenced by their cross section,  $A$ , and therefore, the stress levels were not precisely the expected in all the specimens. All the specimens were instrumented with two TML strain-gauges, type BFLA-5-3-3L, with a 5 mm measuring length, installed precisely at the geometric centre of each face (Figure 3b). A control specimen was monitored simultaneously to subtract any external noise recorded. The tests revealed that the material characteristics distribution is not as uniform as expected, since opposite strain-gauges presented relatively different levels of strain (Figure 4), and for that reason the parameters of the curves were obtained from the average strain value measured in each specimen. Observing the information given in Figure 2b and taking into account the obtained experimental results, it is evident that the shape of Burgers model is the one that more resembles these results.

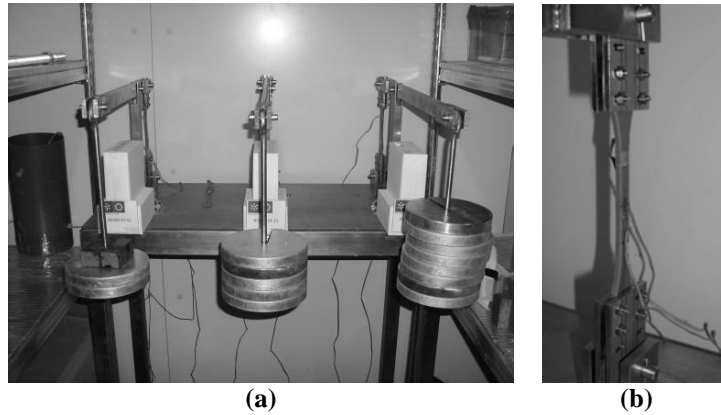


Figure 3 – Experimental setup: (a) creep table, and (b) aspect of an instrumented specimen.

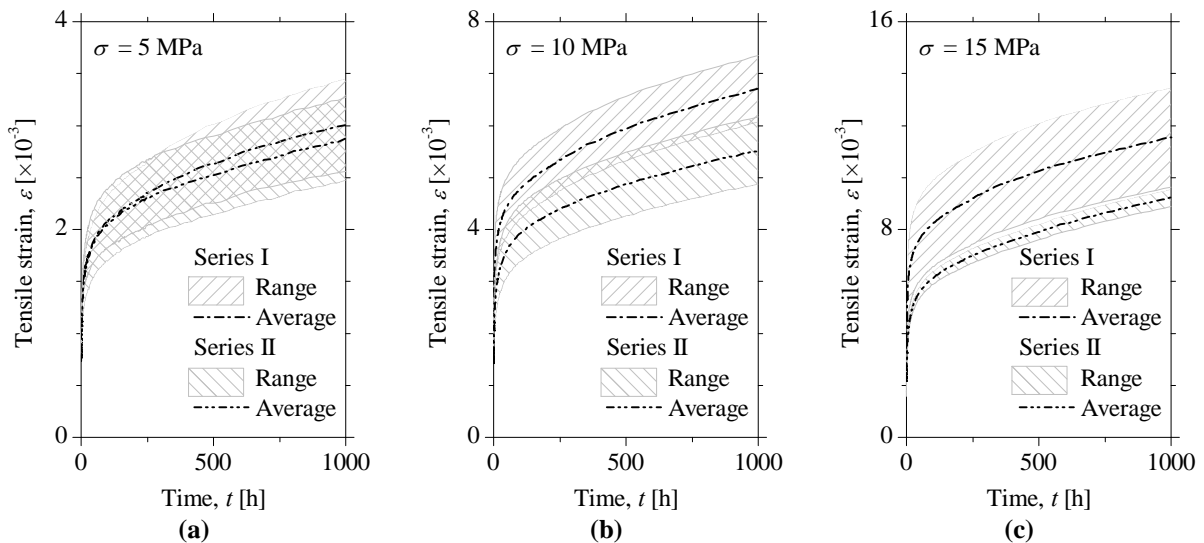


Figure 4 – Experimental tensile creep curves: (a) 5 MPa, (b) 10 MPa, and (c) 15 MPa.

### 3.3 Curve parameters

From the average strain curves, the values of the model parameters were determined as follows (Figure 2b):

- $\varepsilon_M$ , the instantaneous strain mobilized, corresponds to the strain at the instant  $t = 0$ ;
- $\varepsilon'_M$ , the long-term strain velocity that was fixed to be the average slope from  $t = 666.7 \sim 1000$  h;
- $\varepsilon_{eq}$ , the equivalent initial strain that is the value in the strain axis intercepted by the line that

defines  $\varepsilon'_M$ ;

-  $t^*$  is the retardation time that is, by definition, the time necessary to achieve approximately 63% of Kelvin's maximum strain.

The values obtained by this process are presented in Table 2. However, to determine  $t^*$  the process is not so direct and the experimental curve had to be deconstructed using the parameters obtained meanwhile and according to Eq. (2). The result correspondent to this deconstruction is depicted in Figure 5. The rheological parameters necessary to Eq. (1) can at this point be easily obtained by performing basic calculations, and are presented in Table 3.

$$\% \varepsilon_K = \left( 1 - e^{-\frac{E_K t}{\eta_K}} \right) = \frac{E_K}{\sigma} \varepsilon(t) - \frac{E_K}{E_M} - \frac{E_K t}{\eta_M} \quad (2)$$

**Table 2. Notable tensile creep points.**

| SERIES    | $\sigma$<br>[MPa] | $A$<br>[mm <sup>2</sup> ] | $\varepsilon_M$<br>[ $\times 10^{-3}$ ] | $\varepsilon'_M$<br>[ $\times 10^{-3}$ /h] | $\varepsilon_{eq}$<br>[ $\times 10^{-3}$ ] | $t^*$<br>[h] |
|-----------|-------------------|---------------------------|---|--|--|--------------|
| Series I  | 5.1               | 41.697                    | 0.8037                                  | 6.5788E-04                                 | 2.3521                                     | 34           |
|           | 10.0              | 41.234                    | 1.5510                                  | 1.4325E-03                                 | 5.2785                                     | 17           |
|           | 15.4              | 41.472                    | 2.4226                                  | 2.4174E-03                                 | 9.1430                                     | 16           |
| Series II | 5.0               | 42.471                    | 0.7307                                  | 6.5702E-04                                 | 2.2152                                     | 23           |
|           | 9.7               | 42.507                    | 1.4251                                  | 1.2196E-03                                 | 4.3048                                     | 25           |
|           | 15.0              | 42.672                    | 2.1697                                  | 2.4155E-03                                 | 6.8168                                     | 29           |

**Table 3. Rheological parameters.**

| SERIES    | $\sigma$<br>[MPa] | $E_M$<br>[GPa] | $\eta_M$<br>[GPa·h] | $E_K$<br>[GPa] | $\eta_K$<br>[GPa·h] | $n$  |
|-----------|-------------------|----------------|---------------------|----------------|---------------------|------|
| Series I  | 5.1               | 6.39           | 7803                | 3.32           | 113                 | 0.56 |
|           | 10.0              | 6.46           | 6991                | 2.69           | 45                  | 0.61 |
|           | 15.4              | 6.35           | 6363                | 2.29           | 36                  | 0.63 |
| Series II | 5.0               | 6.90           | 7671                | 3.40           | 78                  | 0.53 |
|           | 9.7               | 6.82           | 7966                | 3.37           | 85                  | 0.56 |
|           | 15.0              | 6.89           | 6189                | 3.22           | 93                  | 0.57 |

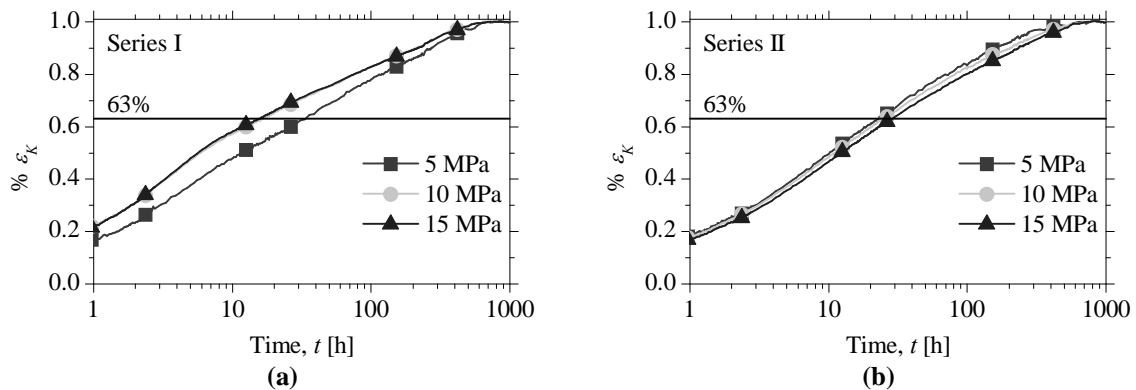


**Figure 5 – Percentage of Kelvin's maximum strain: (a) Series I, (b) Series II.**

Performing a direct substitution of the rheological parameters included in Table 3 in Eq. (1), the strain versus time is predicted with reasonable accuracy. However, in the initial transient

branch, the simulation is not quite accurate (see Figure 6). By curve fitting, Burgers equation was slightly modified, according to bibliographic research findings. Feng *et al.* [8] explained in their work that the presence of moisture can assist molecular mobility and, therefore, decrease the amount of energy required to deform the material and so, they adapted the original form of Burgers model according to Eq. (3). The parameter  $n$  was therefore included in the analytical formulation and estimated to minimize the difference between analytical and experimental curve, producing a much more accurate projection, as depicted in Figure 7.

$$\varepsilon(t) = \frac{\sigma}{E_M} + \frac{\sigma}{\eta_M} t + \frac{\sigma}{E_K} \left( 1 - e^{-\left(\frac{E_K t}{\eta_K}\right)^{1-n}} \right) \quad (3)$$

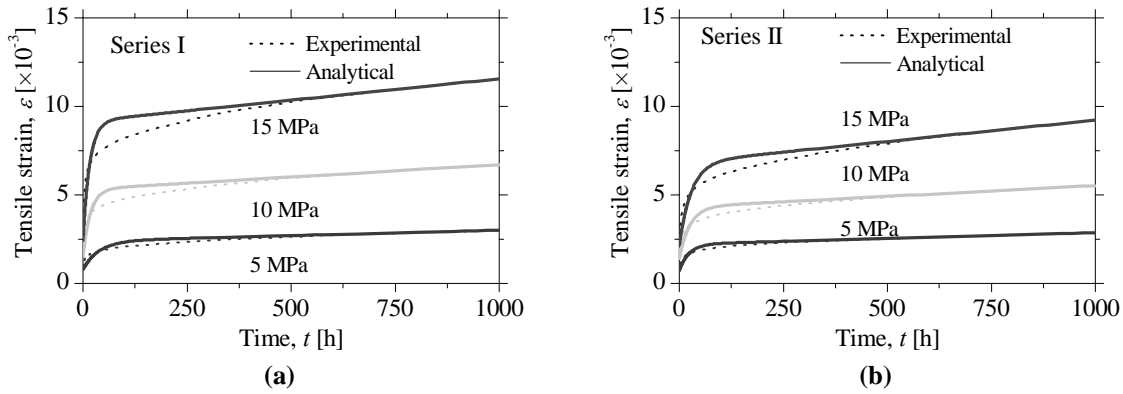


**Figure 6 – Analytical curves obtained by direct substitution (a) Series I and (b) Series II.**

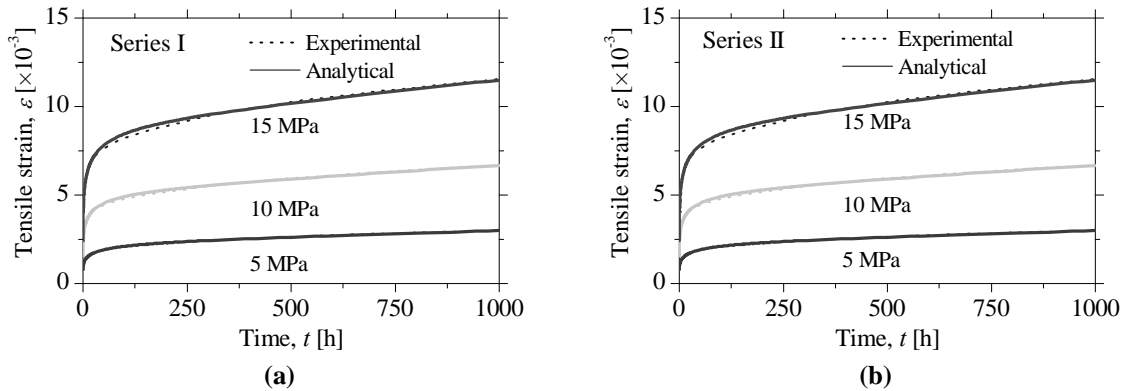


**Figure 7 – Analytical curves obtained by including the parameter  $n$ : (a) Series I, and (b) Series II.**

Analysing the parameters obtained, indicated in Table 3, it is noticed that in the two series of tests performed the adoption of linear relationships for the elastic elements, as illustrated previously in Figure 1a, leads to satisfactory results (Figure 8). It is also verified that the Young modulus obtained in the control tensile tests (Table 1) is smaller than the ones obtained in the linear regression (Figure 8), which is expectable, since the loading process of the creep tests was rather quick. Apart from that slight difference of values, the values of Young modulus between both series are compatible with the control tensile tests, confirming that series II specimens were stiffer than the ones tested in Series I. Concerning the equivalent initial strain,  $\varepsilon_{eq}$ , the linear regression fitting procedure also provided a very good r-square value (Figure 9). These outcomes clearly indicate that for this structural epoxy adhesive both elastic components, denoted in Burgers model as  $E_M$  and  $E_K$ , are constant, regardless the stress level. Additionally, the tests performed show that in Series I the equivalent long-term modulus,  $E_{eq}$ , was approximately 27.5% of the instantaneous modulus,  $E_M$ , while in Series II

this relation was of about 32.3%, which means that the creep factor ( $\phi = E_M / E_{eq} - 1$ ) is about 2.4 at 1000 h. Analysing the viscous components ( $\varepsilon'_M$  in Table 2), it was noticed that although the linear regression showed relatively good performance (Figure 10), a smaller  $r^2$  was obtained than for  $\eta_K$ , which many indicate that it is dependent of the applied stress level. To better illustrate this occurrence the plot on Figure 10 relates the tensile strength ratio ( $\sigma / f_{max,t=1000\text{ h}}$ , where  $f_{max,t=1000\text{ h}}$  is the maximum tensile strength at 1000 h) and the strain velocity,  $\varepsilon'_M$ . Regarding Kelvin's dashpot, is not possible to construct the elementary stress vs. strain velocity plot since the strain velocity is constantly changing in the first loading hours. Furthermore, observing the results previously shown in Table 3, the values of  $\eta_K$  increased with the applied stress in Series I, while in Series II decreased, which is quite contradictory, and about these values, nothing could be concluded, which recommends further research in this topic.

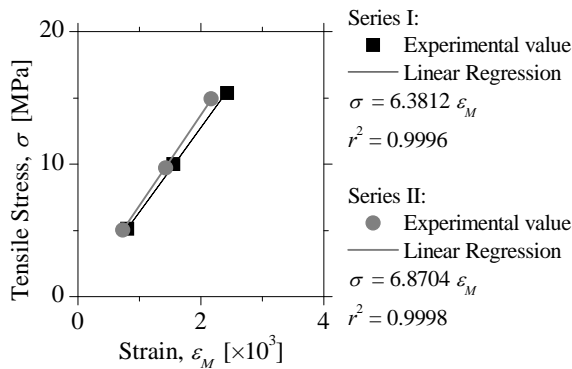


Figure 8 – Stress vs. initial strain relationship.

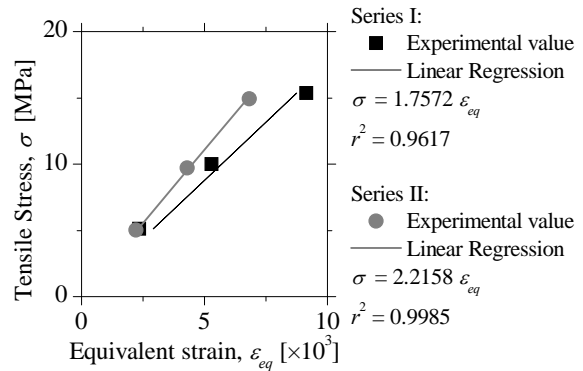


Figure 9 – Stress vs. equivalent strain relationship.

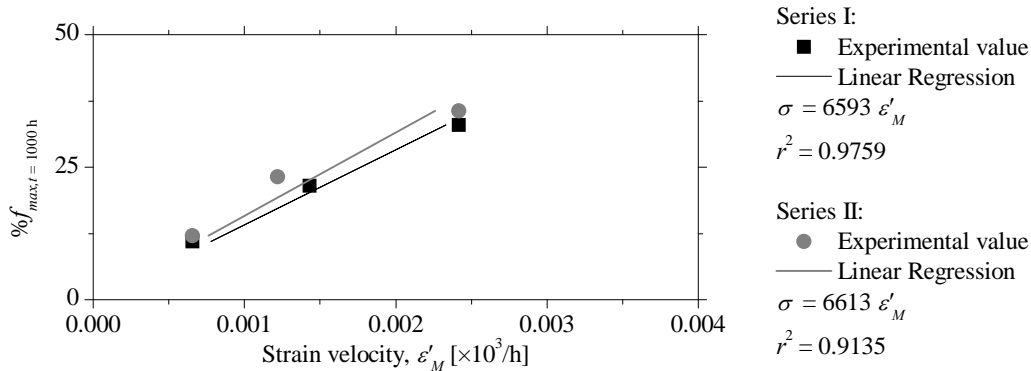


Figure 10 – Stress vs. strain velocity relationship.

## 4. Conclusions

In this paper the most noteworthy theoretical models existent to describe the time-dependent behaviour of structural adhesives are presented. An experimental program that observed the existent standards on creep behaviour was carried out to assess the creep behaviour of a selected commercial structural epoxy adhesive. The tests performed showed that the instantaneous and time dependent properties of the tested adhesive can be observed as roughly constant (under constant temperature and humidity) if the applied stress levels are under 50% of the material's tensile strength. The parameter associated with the initial branch of  $\varepsilon(t)$ ,  $\eta_K$ , seems to be dependent on the applied stress level, but its influence on the long term behaviour of the material is relatively small. This happens because if a period of loading, much greater than 1000 h is considered, the initial accommodation of strains becomes insignificant and, eventually, simplifying the behaviour to a linear model can be a proper

approach. It is suggested to use a rheological model similar to the one proposed by Maxwell, using for initial deformation the value herein identified as equivalent strain,  $\varepsilon_{eq}$ , and for long term deformation increment the value of  $\eta_M$ . Both values can be obtained for any material by creep tests similar to the ones reported, and this approach can later reveal valuable in future numerical simulations. The creep coefficients observed are within the range of values usually observed in concrete specimens (between 1.5 and 3.0), but additional experimental tests should be performed not only to increase the reliability of the results, but also to assess the effect of other environmental conditions.

## 5. Acknowledgements

The first Author acknowledges the support provided by FCT grant, SFRH/BD/61756/2009. The research carried out is part of the project PreLami, with the reference PTDC/ECM/114945/2009. The authors would also like to acknowledge the support provided by HILTI, for supplying the adhesives for the experimental program.

## 6. References

- [1] WIGHT, R.G., GREEN, M.F., ERKI, M-A., "Prestressed FRP Sheets for Poststrengthening Reinforced Concrete Beams", *Journal of Composites for Construction*, Vol. 5, No. 4, 2011, pp. 214-220.
- [2] NORDIN, H., TÄLJSTEN, B., "Concrete Beams Strengthened with Prestressed Near Surface Mounted CFRP", *Journal of Composites for Construction*, Vol. 10, No. 1, 2006, pp. 60-68.
- [3] GAAFAR, M.A., EL-HACHA, R., "Concrete Beams Strengthened with Prestressed Near Surface Mounted CFRP", *International Conference on FRP Composites in Civil Engineering*, 2008, 6 pp.
- [4] LOPEZ-ANIDO, R.A., NAIK, T.R., "Emerging Materials for Civil Engineering Infrastructure - State of the Art", *ASCE Press*, 2000.
- [5] SAYED-AHMED, E.Y., SHRIVE, N.G., "A new steel anchorage system for post-tensioning applications using carbon fibre reinforced plastic tendons." *Canadian Journal of Civil Engineering*, Vol. 25, No. 1, 1998, pp. 113-127.
- [6] LI, C., POTTER, K., WISNOM, M.R., STRINGER, G. "In-situ measurement of chemical shrinkage of MY750 epoxy resin by a novel gravimetric method", *Composites Science and Technology*, Vol. 64, No. 1, 2004, pp. 55-64.
- [7] YU, H., MHAISALKAR, S., WONG, E., "Cure shrinkage measurement of nonconductive adhesives by means of a thermomechanical analyzer", *Journal of Electronic Materials*, Vol. 38, No. 4, 2005, pp. 1177-1182.
- [8] FENG, C.W., KEONG, C.W., HSUEH, Y.P., WANG, Y.Y.; SUE, H.J. "Modeling of long-term creep behavior of structural epoxy adhesives", *International Journal of Adhesion & Adhesives*, Vol. 25, No. 5, 2005, pp. 427-436.
- [9] COSTA, I.G., BARROS, J.A.O., "Creep of Adhesives - Review", *Technical Report*, No. 11-DEC/E-03, 2011, 39pp.
- [10] ASTM 2990, "Standard Test Methods for Tensile, Compressive, and Flexural Creep and Creep-Rupture of Plastics" *American Society for Testing and Materials*, 2001.
- [11] ISO 899-1, "Plastics - Determination of creep behaviour - Part 1: Tensile creep" *International Organization for Standardization*, 2003.
- [12] BRINSON, H.F., BRINSON, L.C., "Polymer Engineering Science and Viscoelasticity: An Introduction." *Springer Science & Business Media*, 2008.
- [13] ISO 527-2, "Plastics - Determination of tensile properties - Part 2: Test conditions for moulding and extrusion plastics" *International Organization for Standardization*, 1993.